Exchange bias effect in CaMn1-xRexO3

V. Markovich, I. Fita, A. Wisniewski, R. Puzniak, Christine Martin, G. Jung, G. Gorodetsky

Exchange bias effect in $CaMn_{1-x}Re_{\#\#}O_3$

Cite as: AIP Advances **7**, 055801 (2017); https://doi.org/10.1063/1.4972798
Submitted: 31 August 2016 • Accepted: 22 September 2016 • Published Online: 20 December 2016

V. Markovich, I. Fita, A. Wisniewski, et al.

Exchange bias effect in $CaMn_{1-x}Re_xO_3$

V. Markovich,[1,a] I. Fita,[2] A. Wisniewski,[2] R. Puzniak,[2] C. Martin,[3] G. Jung,[1,2] and G. Gorodetsky[1]

[1]*Department of Physics, Ben-Gurion University of the Negev, 84105 Beer-Sheva, Israel*
[2]*Institute of Physics, Polish Academy of Sciences, PL-02668 Warsaw, Poland*
[3]*Laboratoire CRISMAT, UMR 6508, ISMRA, 14050 Caen Cedex, France*

(Presented 2 November 2016; received 31 August 2016; accepted 22 September 2016; published online 20 December 2016)

Exchange bias effect in $CaMn_{1-x}Re_xO_3$ ($x \leq 0.1$) has been investigated. The effect is very small in the samples doped at $x = 0.02$ and 0.04, but increases monotonously with further increase in Re doping. For $x = 0.1$, both vertical and horizontal shifts in hysteresis loop of field cooled sample decrease monotonously with increasing temperature and vanish above 70 K, while coercivity disappears only above 90 K upon approaching the Néel temperature. Exchange bias field, coercivity, and remanence asymmetry depend sensitively on temperature and maximal measuring field. Magnetic training effect has been studied for $x = 0.06$, 0.08, 0.1 samples and analyzed using a spin relaxation model. The observed exchange bias is attributed to the low-temperature phase separation into ferromagnetic clusters and the *G*-type and/or *C*-type antiferromagnetic matrix. [http://dx.doi.org/10.1063/1.4972798]

The exchange bias (EB) phenomenon, discovered by Meiklejohn and Bean,[1] has been intensively studied because of its importance for the magnetic information storage technologies.[2–5] Usually, the EB effect manifests itself by shifts in the isothermal magnetization vs applied field curves along the field direction and sometimes along the magnetization axis, as well as by an enhancement of the coercive field H_C in the field cooled (FC) process. In general, the EB results from coupling between ferromagnetic (FM) spins and interfacial, uncompensated antiferromagnetic (AFM) spins, occurring during cooling of a FM-AFM system through the Néel temperature in applied magnetic field. After the first observation of the EB effect in $Pr_{1/3}Ca_{2/3}MnO_3$ manganite by Niebieskikwiat and Salamon,[6] it has been reported for various phase-separated manganites and cobaltites.[5,7–9]

The parent $CaMnO_3$ manganite is the *G*-type antiferromagnet in which the spin of Mn^{4+} ion is antiparallel to the spins of the six nearest neighbor Mn^{4+} ions. The Néel temperature T_N of $CaMnO_3$ may vary in the range 110–130 K, depending on the concentration of oxygen vacancies.[10,11] Doping of Mn sites with metal atoms with valance > 4+ creates Mn^{3+} ions and induces FM clusters in the AFM matrix.[12] It was found that the occurrence of EB depends strongly on relative ratio of volumes of FM clusters and AFM matrix. Noticeable EB appears in the systems with small volume of FM clusters.[8] Our recent study[13] on magnetic properties of Re-doped $CaMn_{1-x}Re_xO_3$ (CMRO) ($0 \leq x \leq 0.1$) suggested that the ground state evolves with increasing x, from the *G*-type AFM state with weak FM component (for x up to 0.06) to mostly *C*-type AFM state with charge ordering for $x = 0.08$ and 0.1.

In this paper, we report on EB effect in CMRO system. In particular we report on the temperature dependence of hysteresis loops in various maximal magnetic fields H_{MAX}, up to 50 kOe and on training effect (TE) for $x = 0.06$, 0.08 and 0.1 samples.

In our studies, we have employed polycrystalline samples prepared by a standard ceramic route in air, with intermediate crushing and heating.[12] The magnetic measurements and X-rays diffraction data have shown that CMRO samples are paramagnetic (PM) with *Pnma* crystallographic symmetry

[a]Corresponding Author Vladimir Markovich: markoviv@bgu.ac.il

at room temperature.[13] Magnetic measurements were performed using PAR 4500 vibrating sample magnetometer in magnetic field ≤ 15 kOe, while dc magnetization measurements at higher magnetic field were carried out using the vibrating sample magnetometer (VSM) option of Quantum Design Physical Property Measurement System.

Temperature dependences of the field cooled and zero field cooled magnetization, M_{FC} and M_{ZFC}, of $CaMn_{1-x}Re_xO_3$ ($0.04 \le x \le 0.1$), recorded at applied field of 100 Oe, are shown in Fig. 1(a), while those for $x = 0.02$ sample are shown in the inset to Fig. 1(a). Magnetization at temperatures above 110 K is very small for all studied samples. Low temperature magnetization for the sample with $x = 0.1$ remains very low while that for the sample with x up to 0.08 varies non-monotonously with x. The temperature evolution of M_{FC} and M_{ZFC} demonstrates that: (i) T_N, associated with increase of M_{FC}, decreases with increasing x from ~ 110 K at $x = 0.04$ to ~ 95 K at $x = 0.1$. (ii) M_{FC} and M_{ZFC} of all studied samples considerably split below T_N, indicating the presence of frustrated magnetic states. (iii) M_{FC} and M_{ZFC} for the sample with $x = 0.02$ exhibit a maximum below T_N and then change the sign and become negative at $T < 40$ K.

Low temperature M_{FC} recorded at $H = 15$ kOe (Fig. 1(b)) increases with increasing x up to $x = 0.04$ and decreases with further increase in x. In the PM range, $150 < T < 250$ K, M_{FC} increases with increasing doping for $0.02 \le x \le 0.08$, while M_{FC} at $x = 0.1$ almost coincides with that at $x = 0.08$. Field cooled magnetization of the latter samples exhibits wide maximum related to the charge/orbital ordering (CO/OO) at $T_{CO} \approx 121$ K for the sample with $x = 0.08$ and $T_{CO} \approx 139$ K for that with $x = 0.1$. Inset to Fig. 1(b) shows magnetic hysteresis loops measured at $T = 10$ K after ZFC. The spontaneous magnetization M_0, evaluated by linear extrapolation of the high field magnetization

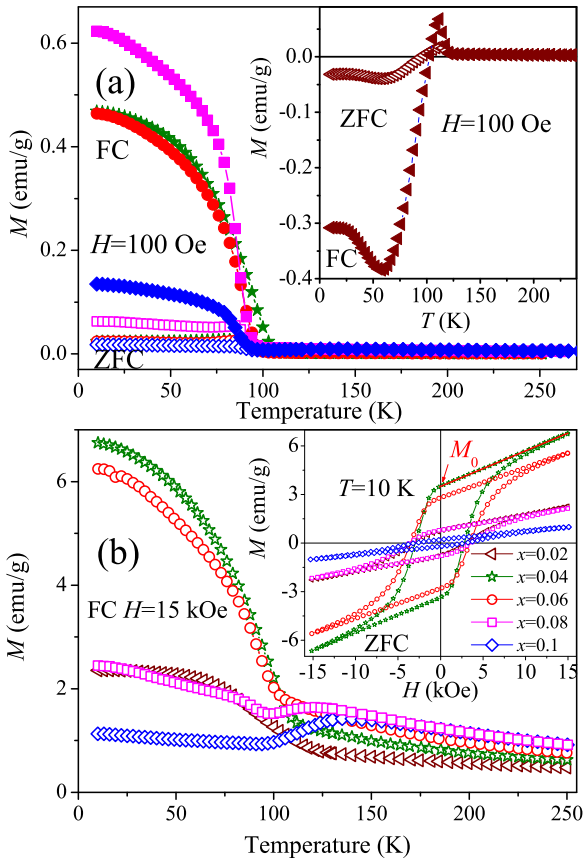

FIG. 1. (a) and inset in (a) $M_{ZFC}(T)$ (open symbols) and $M_{FC}(T)$ (solid symbols) recorded in $H = 100$ Oe for $CaMn_{1-x}Re_xO_3$ samples with $x = 0.02$ (triangles), $x = 0.04$ (stars), $x = 0.06$ (circles) $x = 0.08$ (squares), $x = 0.1$ (diamonds). (b) $M_{FC}(T)$ recorded in magnetic field of $H = 15$ kOe. Inset shows hysteresis loops for $CaMn_{1-x}Re_xO_3$ samples recorded at $T = 10$ K after ZFC. (b) Hysteresis loops of CMRO at various T, as measured after FC in $H_{cool} = 15$ kOe.

to $H = 0$, is very small (0.79 emu/g) for $x = 0.02$, increases quickly with increasing x, peaks at $x = 0.04$ ($M_0 \approx 3.53$ emu/g), and then drops to 0.24 emu/g for $x = 0.1$. Small values of $M_0(x)$ indicate that at low temperatures, the major part of the magnetic volume of CMRO samples is occupied by AFM matrix.

Figure 2(a) shows hysteresis loops measured at various temperatures for the sample with $x = 0.1$ after FC in $H_{cool} = 15$ kOe. There is no magnetic hysteresis above 100 K. Loops recorded at $T < 80$ K show shifts along magnetic field axis which is absent in the ZFC loops, as expected for the EB effect. This shift of the hysteresis loop is usually quantified as $H_{EB} = -(H_1+H_2)/2$, where H_1 and H_2 are the fields at which the magnetization equals zero for decreasing and increasing branch of the loop, respectively.[1–5] The shift along the magnetization axis is quantified as $M_{EB} = (M_1+M_2)/2$, where M_1 and M_2 are the magnetizations at $H = 0$ for decreasing and increasing branches of the hysteresis loop, respectively. The presence of a vertical shift can be linked to the remanent state, arising from the presence of a FM-like phase distributed in the AFM matrix. It appears that H_{EB} is very small for the sample with $x = 0.02$ and 0.04, and increases with increasing doping at $x > 0.04$, as the volume of FM phase decreases. Therefore, we have studied in details the EB effect only for higher doping levels, $x = 0.06$, 0.08, and 0.1.

For maximal applied magnetic field $H_{MAX} = 15$ kOe, the magnetization is far from being saturated. The ascending and descending branches of hysteresis loops coincide only at fields close to the H_{MAX}. Thus, the observed H_{EB} and M_{EB} may represent somewhat the effect of minor loops.[14–16] It was suggested that the presence of the "true" EB may be derived only from effectively saturated hysteresis loops recorded in high enough H_{MAX}.[14–16] A system will be considered effectively saturated if the ascending and descending branches of its hysteresis loop coincide at fields higher than the anisotropy field.

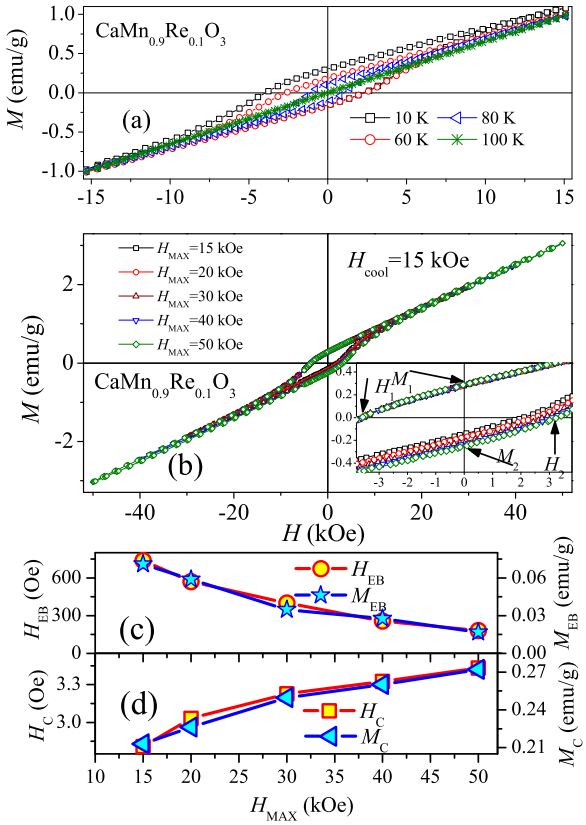

FIG. 2. (a) Hysteresis loops of $x = 0.1$ sample, at various T, as measured after FC in $H_{cool} = 15$ kOe. (b) Hysteresis loops of $x = 0.1$ sample as measured at $T = 10$ K after FC in $H_{cool} = 15$ kOe with different H_{MAX}. (c,d) H_{EB}, M_{EB}, H_C, and M_C as a function of H_{MAX}.

To verify if the EB in CMRO is an intrinsic one, we have investigated the dependence of H_{EB} and M_{EB} on H_{MAX} for the sample doped at $x = 0.1$. It can be seen in Fig. 2(b) that for low H_{MAX}, loops exhibit large horizontal and vertical shifts. However, for the same cooling field H_{cool} and large enough H_{MAX}, H_{EB} and M_{EB} stabilize, see Fig. 2(c). It appears that H_{EB} and M_{EB} decrease with increasing measuring field H_{MAX} in very similar manner, while H_C and M_C increase with increasing field, see Fig. 2(d). Here, the coercivity H_C is defined as the half-width of the loop $H_C = (H_2 - H_1)/2$, while the magnetic coercivity $M_C = (M_1 - M_2)/2$ is the "vertical axis" equivalent of H_C.

The essential property of any exchange biased system is so-called training effect, which manifests itself in the reduction of H_{EB} with increasing number of consecutively recorded loops at a fixed temperature.[3,5,9] We have measured 10 hysteresis loops for $x = 0.06$, 0.08, and 0.1 samples at $T = 10$ K after FC at $H_{cool} = 20$ kOe with $H_{MAX} = 50$ kOe. It is well known that H_{EB} change is the most significant between the first and the second loop.[3,5,9] Moreover, the change is the most pronounced at the left branch of the loop, while the right branch evolves only slightly. Figure 3(a) shows the recording of 10 hysteresis loops for $x = 0.1$ sample, while Fig. 3(b) presents an enlarged view of the shift in the left branch of $M(H)$. The loops shift toward lower fields upon increasing number of field cycles n. Figure 3(c) shows the dependence of both H_1 and H_2 on the number n of field cycles, while the evolution of H_{EB} with n is presented in Fig. 3(d). The dependence of H_{EB} on the number of cycles n can be well fitted by a simple power law expression,[3,5,9]

$$H_{EB}(n) - H_{EB\infty} \propto A/\sqrt{n}, \tag{1}$$

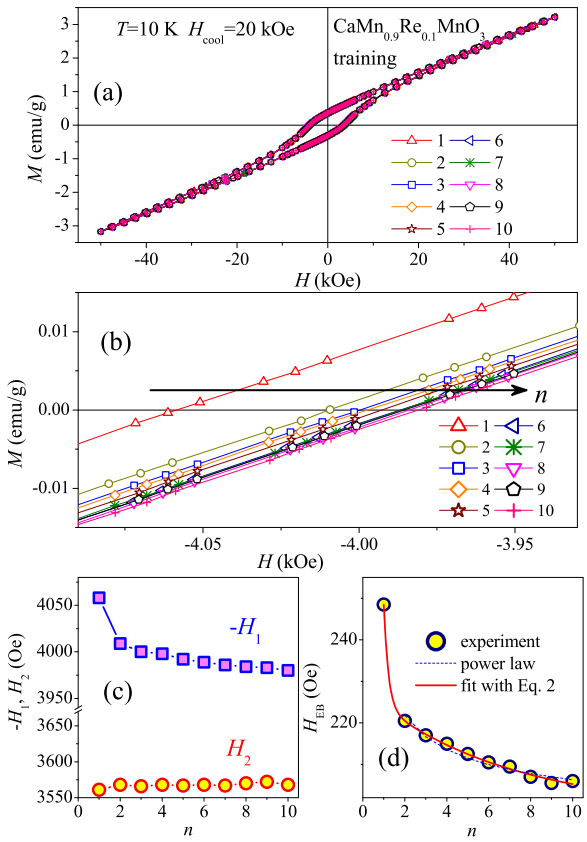

FIG. 3. (a) Consecutively measured ten hysteresis loops of the sample with $x = 0.1$ at $T = 10$ K cooled under $H_{cool} = 20$ kOe with $H_{MAX} = \pm 50$ kOe. (b) The enlarged view of these loops to reveal the shift of the loops with increasing loop number. (c) Variation of the coercive fields H_1 and H_2 with number of recurrent hysteresis loops n. (d) The symbols represent the experimental data for H_{EB} versus loop index number. Dashed line corresponds to a fit with a power law (Eq. (1)) for $n \geq 2$, while solid line illustrates the best fit with the Eq. (2).

TABLE I. Values of expressions 1 and 2 fitting parameters approximating experimental data for TE.

$H_{EB}(n) = H_{EB\infty} + A_f \exp(-n/P_f) + A_i \exp(-n/P_i)$						
sample	$H_{EB\infty}$(Oe)	A_f (Oe)	P_f	A_i (Oe)	P_i	R^2
x=0.06	39±4	110±20	0.4±0.1	9±2	6±3	0.983
x=0.08	78±3	56000±8000	0.1±0.1	12±2	6±2	0.987
x=0.1	199±5	2000±1000	0.2±0.1	29±2	7±3	0.998
$H_{EB}(n) - H_{EB\infty} \propto A/\sqrt{n}$						
sample	$H_{EB\infty}$ (Oe)		A (Oe)		R^2	
x=0.06	36.7±0.6		14±2		0.936	
x=0.08	70.1±0.8		17±2		0.954	
x=0.1	194±2		40±3		0.963	

where $H_{EB\infty}$ is the value of the EB field recorded at $n \to \infty$. The dashed line in Fig. 3(d) shows the best fitted curve for $n \geq 2$ with $H_{EB\infty}$ = 194 ± 2 Oe. Fitting parameters for all doping levels are presented in Table I. It should be underlined that the relation (1) holds only for $n \geq 2$ and cannot explain steep relaxations between the first and the second loop.

Recently, the TE has been alternatively described using two different relaxation rates for frozen and rotatable uncompensated spin components at the interface.[17] In this approach

$$H_{EB}(n) = H_{EB\infty} + A_f \exp(-n/P_f) + A_i \exp(-n/P_i), \quad (2)$$

where A_f and P_f are related to changes in the frozen spins configuration, and A_i and P_i are evolving parameters linked to the rotatable spin component at the FM/AFM interface. The magnetic field dimension is dimension of parameters A, while parameters P are dimensionless and in some sense act as a relaxation time, although the continuous time variable is replaced by a discrete loop number. Equation (2) fits to the data much better than the simple power law, including the first two points, as proved by the fitting quality parameter R^2. The relevant fitting parameters are shown in Table I. It appears that for all studied samples the contributions of rotatable uncompensated AFM spins and frozen AFM components at the interface are comparable at the initial stage of the training but the frozen AFM component relaxes much slower with respect to the rotatable one. Indeed, the rotatable uncompensated AFM spins relax much quicker for higher doped samples ($x = 0.08$ and 0.1) and their contribution becomes vanishingly small already at $n = 2$, while for $x = 0.06$ the rotatable contribution remains still essential for $n = 2$. The difference in the relaxation of both components may be measured by the relative rate of relaxation of frozen and rotatable spins P_f / P_i which for the sample with $x = 0.06$ is significantly larger than that for the samples with higher doping levels. In principle, that difference may be a consequence of differences in phase separation in different samples. We have recently proposed that small FM clusters are distributed in the G-type AFM matrix for $x = 0.06$ case, while and in samples with $x = 0.08$ and 0.1, the matrix is more anisotropic C-type CO AFM.[13] Unfortunately, significant errors in the fitting parameters do not enable us to confirm such a claim in this case. We may only conclude that Eq. (2) describes well the TE effect in studied samples.

This work was supported by the Polish NCN grants 2014/15/B/ST3/03898 and 2012/05/B/ST3/03157.

[1] W. H. Meiklejohn and C. P. Bean, Phys. Rev. **102**, 1413 (1956); **105**, 904 (1957); W. H. Meiklejohn, J. Appl. Phys. **33**, 1328 (1962).
[2] J. Nogués and I. K. Schuller, J. Magn. Magn. Mater. **192**, 203 (1999).
[3] J. Nogués, J. Sort, V. Langlais, V. Skumryev, S. Suriñach, J. S. Muñoz, and M. D. Baró, Phys. Rep. **422**, 65 (2005).
[4] F. Radu and H. Zabel, in *Magnetic Heterostructures: Advances and Perspectives in Spin structures and Spin transport*, Ed. H. Zabel and S. D. Bader, Springer Tracts in Modern Physics (Springer-Verlag, Berlin, 2008), vol. 227, pp. 97–184.
[5] S. Giri, M. Patra, and S. Majumdar, J. Phys.: Condens. Matter. **23**, 073201 (2011).
[6] D. Niebieskikwiat and M. B. Salamon, Phys. Rev. B **72**, 174422 (2005).
[7] T. Qian, G. Li, T. F. Zhou, X. Q. Xiang, X. W. Kang, and X. G. Li, Appl. Phys. Lett. **90**, 012503 (2007).

[8] I. Fita, V. Markovich, A. Wisniewski, R. Puzniak, C. Martin, V. N. Varyukhin, and G. Gorodetsky, Phys. Rev. B **88**, 064424 (2013).
[9] S. Karmakar, S. Taran, E. Bose, B. K. Chaudhuri, C. P. Sun, C. L. Huang, and H. D. Yang, Phys. Rev. B **77**, 144409 (2008).
[10] J. B. MacChesney, H. J. Williams, J. F. Potter, and R. C. Sherwood, Phys. Rev. **164**, 779 (1967).
[11] E. O. Wollan and W. C. Koehler, Phys. Rev. **100**, 545 (1955).
[12] B. Raveau, A. Maignan, C. Martin, and M. Hervieu, Mater. Res. Bull. **35**, 1579 (2000).
[13] V. Markovich, I. Fita, A. Wisniewski, R. Puzniak, C. Martin, D. Mogilyansky, G. Jung, and G. Gorodetsky, to be published.
[14] G. Salazar-Alvarez, J. Sort, S. Suriñach, M. D. Baró, and J. Nogués, J. Am. Chem. Soc. **129**, 9102 (2007).
[15] J. Geshev, J. Magn. Magn. Mater. **320**, 600 (2008); J. Phys.: Condens. Matter **21**, 078001 (2009); J. Appl. Phys. **105**, 066108 (2009).
[16] A. Harres, M. Mikhov, V. Skumryev, A. M. H. de Andrade, J. E. Schmidt, and J. Geshev, J. Magn. Magn. Mater **402**, 76 (2016).
[17] S. K. Mishra, F. Radu, H. A. Dürr, and W. Eberhardt, Phys. Rev. Lett. **102**, 177208 (2009).